Nanovoids in MBE-grown SiGe alloys implanted *in situ* with Ge^+ ions

P. I. Gaiduk,* J. Lundsgaard Hansen, and A. Nylandsted Larsen
Department of Physics and Astronomy, University of Aarhus, DK-8000, Aarhus C, Denmark

E. A. Steinman
Institute of Solid State Physics, RAS, 142432, Moscow distr., Chernogolovka, Russia
(Received 5 July 2002; revised manuscript received 7 October 2002; published 11 June 2003)

Spherically shaped voids, of nanometer size, are observed in molecular-beam epitaxially grown SiGe alloy layers implanted *in-situ* at elevated temperature with low-energy Ge ions, followed by thermal treatments. The voids are exclusively assembled in the narrow, implanted band. The voids only appear in the layers after a heat treatment at a temperature higher than 700 °C, and they are stable up to 900 °C. Arsenic ion implantation at similar conditions does not give rise to void formation but to regular interstitial dislocation loops. The nucleation stage of the voids is accompanied by a strong photoluminescence-yield enhancement in the range of 1.4–1.55 μm, originating from the strained SiGe alloy layer which contain vacancy clusters or small voids.

DOI: 10.1103/PhysRevB.67.235310 PACS number(s): 61.72.Qq, 61.72.Ji, 61.72.Ff, 81.15.Hi

I. INTRODUCTION

Effective light emission from crystalline silicon is a crucial step in the development of silicon-based optoelectronics. Due to its indirect band gap, bulk Si does not exhibit any remarkable light emission and has been, for that reason, considered inappropriate for optoelectronics. Much effort, however, has been recently devoted to overcoming this fundamental property of Si and to achieving effective room-temperature luminescence. In particular, the physical properties and optical performance of various silicon-related and silicon-compatible materials (nanocrystals,[1] Si and Ge nanodots in SiO_2,[2] porous Si,[3] Er-doped Si,[4] Ge and $Si_{1-x}Ge_x$ quantum dots grown on Si,[5,6] etc.) are under intensive investigation, and clear prospects to develop efficient light-emission devices emerge. On the other hand, the integration of porous Si- or nano-Si(Ge)-SiO_2-based light emitters with VLSI technology is still questionable because of the following reasons: (1) The room temperature luminescence quantum efficiency degrades very fast due to high porosity, fragility, unstable passivation and poor thermal conductivity. (2) The fabrication methods of porous Si formation are not easily compatible with existing VLSI technology. (3) In addition to efficient radiative recombination, electroluminescence (EL) requires electron-hole injection and transport to the active region where the recombination occurs; insulating or porous matrices, however, complicate both efficient carrier injection and production of good-quality contacts.

Another promising roadmap for Si-based light-emitters which is compatible with silicon integrated circuit technology is to use light-emitting dopants (e.g., Er) or defects (dislocations, Ge or SiGe islands, etc.) incorporated in the carrier-depletion zone of bulk Si.[4–9] In particular, efficient EL at room temperature has been reported recently as being due to dislocations in silicon, caused by plastic deformation or strain relaxation in Si and SiGe alloys,[7] by surface melting with a high power focused Ar^+ laser beam,[8] or by ion implantation followed by thermal treatment.[9] A further increase in silicon light-emitting diode power conversion efficiency to values above 1% near room temperature has been demonstrated after an appropriate minimization of the total internal reflection by surface texturing.[10]

Recently, *in situ* implantation of As has been effectively applied for the modification of SiGe buffer layers to enhance the formation of self-assembled Ge nanodots,[6] to grow novel, semi-spherical SiGe nanostructures,[11] and for ion-beam synthesis of self-organized narrow band-gap GeAs nanodots.[12] In particular, we have observed, by transmission electron microscopy, vertically correlated Ge islands molecular beam epitaxy (MBE) grown on a Si/SiGe buffer structure modified by *in situ* ion implantation of 1-keV As or Ge.[6] The enhancement of the Ge-QD (quantum dot) nucleation and formation is found to be due to the formation of a defect band in the buffer layer which causes nanometer-scale undulations and a roughness of the buffer layer, but fortunately does not result in the penetration of dislocations or any other extended defects into the top Ge/Si layers.[6] The clusters of point defects created in the buffer layer during the MBE growth plus implantation stage are unstable and it is natural to expect their evolution into interstitial type dislocation loops[13–15] during an additional annealing. In the present work an *unexpected* evolution of extended defects into nanovoids is demonstrated in the case of Ge *in situ* implantation followed by thermal treatment. It is also shown that a strong increase of the photoluminescence yield takes place during the formation of an array of precisely self-adjusted nanovoids.

II. EXPERIMENTAL PROCEDURE

The samples were grown by solid-source MBE using *e*-beam evaporators for the Si and Ge deposition and a built-in low energy (1 keV) ion implanter for *in situ* incorporation of As or Ge. Wafers of *p*-type (001) Si were used as substrates. Following the SiO_2 desorption from the surface at 850 °C, a 100-nm-thick Si buffer layer was grown. Subsequently, a buffer structure was grown at 525 °C consisting of four alternating layers of 3-nm Si and 2.8-nm $Si_{0.5}Ge_{0.5}$. The growth temperature was controlled using both a pyrometer and a thermocouple, giving a temperature accuracy of about

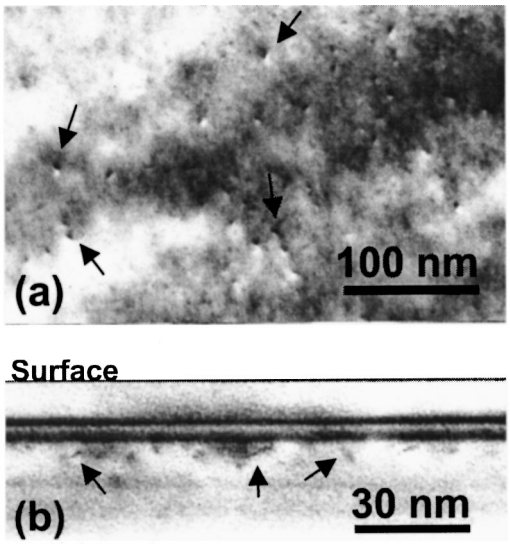

FIG. 1. Bright-field plan-view (a) and cross-section (b) TEM images of as-grown SiGe/Si structure. The arrows indicate some of the extended planar defects.

15°. Typical growth rates were 0.084 and 0.1 Å/s for the Si and $Si_{0.5}Ge_{0.5}$ layers, respectively. During the growth of this four-layered buffer structure, either 1-keV As^+ or Ge^+ ions were implanted *in situ* at a current density of 0.02 μA/cm^2 to a total dose of about 1.6×10^{14} cm^{-2}. The selection of these implanted species was motivated by their neighborhood in the Periodic Table, which assures a similarity in the radiation-defect production. As solutes in silicon, however, their chemical properties (solubility, diffusion, electrical activation, interactions with defects, etc.) are very different. Finally, a 10-nm Si cap layer was deposited. One set of wafers was *in situ* annealed in the MBE chamber at temperatures between 600 and 950 °C for 10 min. Another set was annealed at the same temperatures *ex situ* to the MBE chamber in a furnace for 10 min or by a 30-s rapid thermal annealing (RTA) in N_2 or O_2 ambiances. The layer structures were investigated by transmission electron microscopy (TEM) in both plan-view and cross-section (XTEM) modes, using a Philips CM20 instrument operating at 200 kV. The TEM specimens were thinned down to electron transparency using a procedure consisting of successive mechanical polishing and ion-beam milling at room temperature. Photoluminescence (PL) was excited at 4.2 K by a 488.8-nm line of Ar^+ laser with the excitation power density of about 1 W/cm^2. The PL intensity was measured using a liquid nitrogen cooled Ge photoresistor with an MDR-2 fast monochromator and a conventional lock-in technique.

III. EXPERIMENTAL RESULTS

A typical structure before annealing is presented in Fig. 1 as both plan-view and cross-section images. The layers contain clusters of point defects and a number of extended planar defects along the (001)- and (111)-crystalline planes; some of them are indicated by arrows in Fig. 1. The atomic structure and the nature of these defects are presently under investigation by high-resolution TEM. A ''normal'' way for thermal evolution of ion-implantation induced defects, produced as a result of the above, or similar, implantation conditions, is their transformation into interstitial clusters, rodlike defects and dislocation loops (DLs).[13–15] In our samples, however, annealing above ~750 °C results in an unusual structural transformation: Annealing both in the MBE chamber and in an external furnace results in the formation of a large density (10^9–5×10^{10} cm^{-2}, depending on the thermal treatment regime; see Table I) of circular defects, however no dislocations nor DLs are found in the layer. Figures 2(a) and 2(b) show a matched pair of two-beam, bright-field, underfocused and overfocused TEM micrographs obtained from a thin film in a two-beam diffraction condition with a deviation parameter $s>0$. The defects show minimal contrast at focus. In the underfocused micrograph [Fig. 2(a)] the defects are imaged as bright circles surrounded by Fresnel fringes, whereas in the overfocused micrograph [Fig. 2(b)] they display dark contrast. In dynamical conditions the defects appear bright against dark regions of the extinction con-

TABLE I. The diameter (d_ν) and the areal density (N_ν) of the voids, and the total volume occupied by the voids (C_ν) after *in situ* Ge implantation as a function of temperature (T_a), time (t_a), and ambiance (A) of annealing. The annealings were done in the following ambiances: N_2, dry nitrogen; O_2, dry oxygen; and Vac, in the high vacuum conditions of the MBE chamber. ^{As})- indicates *in situ* As implantation in which case d_ν is the diameter and N_ν the areal density of the dislocation loops.

T_a (°C)	t_a (s)	A	d_ν (nm)	N_ν (cm^{-2})	C_ν (cm^3/cm^2)
750	600	N_2	5–10	$(1.9–2.2)\times10^{10}$	$\sim4.5\times10^{-9}$
750	600	Vac	5–12	$(1.5–1.9)\times10^{10}$	$\sim5.4\times10^{-9}$
800	600	N_2	8–15	$(7–9)\times10^9$	$\sim5.5\times10^{-9}$
900	600	N_2	10–25	$(0.8–1)\times10^9$	$\sim4.2\times10^{-9}$
800	30	N_2	4–9	2.7×10^{10}	$\sim3.9\times10^{-9}$
900	30	N_2	4–10	4×10^9	$\sim5.7\times10^{-9}$
			15–25	1.2×10^9	
900	30	O_2	6–10	8×10^9	$\sim2.2\times10^{-9}$
800^{As})	30	N_2	10–25	1.9×10^{10}	
900^{As})	30	N_2	30–40	3.6×10^9	

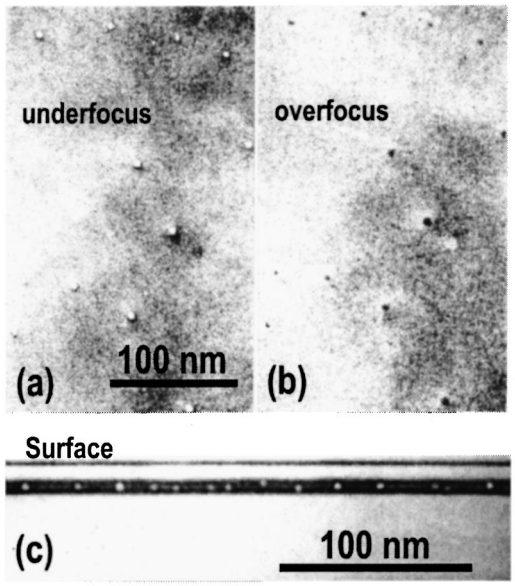

FIG. 2. Bright-field plan-view [(a) and (b)] and cross-section (c) TEM images of the same SiGe/Si structure as in Fig. 1 after furnace annealing at 800 °C for 10 min. The images (a) and (c) are obtained in the conditions of underfocusing. Image (b) is overfocused. The BF TEM images (a) and (b) were obtained in a two-beam diffraction condition with a deviation parameter $s>0$. Note that in (c) the voids are strictly assembled within the SiGe layer.

tour, and dark against bright regions. In the ''out-of-Bragg conditions,'' they keep their circular shape after large inclinations of the sample in the microscope with respect to the electron beam, and they do the same in a cross-section view [Fig. 2(c)]. In accordance with Ref. 16, the above observations demonstrate that the circular defects are open-volume defects or voids. Please note, that during the thermal treatment a strong interdiffusion takes place between the original MBE grown Si and $Si_{0.5}Ge_{0.5}$ layers and, as a result, only one $Si_{1-x}Ge_x$ layer exists after annealing [compare Figs. 1(b) and Fig. 2(c)]. The voids, however, are still solely located within the implanted layer [Fig. 2(c)].

We can exclude that these spherical defects are Ge droplets/precipitates from the following arguments. First, from an energetical point of view precipitation of Ge in Si is of minor importance because Si and Ge are fully miscible and form random substitutional alloys at all compositions. Moreover, despite a sharp compositional interface between bulk Si and Ge dots grown in the Stranski-Krastanow mode at low temperature (550 °C), a very fast interdiffusion and SiGe alloying takes place at temperatures higher than 600–700 °C (see, e.g., Ref. 5). It is therefore straightforward to assume fast alloying at the temperature of annealing (750–950 °C), which is also evidenced by strong interdiffusion between the original MBE grown Si and $Si_{0.5}Ge_{0.5}$ [Fig. 2(c)]. Second, Ge atoms are heavier and larger than Si atoms which results in a difference between the structure factor of the Ge precipitate (hypothetical nanosize Ge particles should be strained) and of the Si matrix, and in a strong strain distribution in the Si matrix around the Ge precipitates. As a consequence, being spherical within the Si matrix, such precipitates should exhibit a sharp black-white contrast in two-beam diffraction conditions.[16] In the TEM images taken far away from any diffraction vector, the deformation contrast will disappear and the defect should have a dark uniform contrast in a gray background, which is a consequence of atoms of higher masses than in the surrounding matrix.[16] In our TEM investigations we were not able to detect the above features and the defects display a minimal contrast in focused conditions. Finally, we were not able to detect any indication of Moire fringes in any diffraction conditions which would have been expected if some large Ge precipitates are strain-relaxed. It should be noted that depending on the regime of RTA, the size of the voids varies from 4 up to 25 nm (see Table I), i.e., in some RTA conditions (e.g., high RTA temperature), the defects are large enough to show most of the above features if they were Ge precipitates.

A general tendency of the thermal evolution of the voids is their increase in size and decrease in density with increasing annealing temperature (Table I). At a given temperature (800–900 °C), with time the voids also grow in size and decrease in density. However, as a function of both temperature and time, the total volume occupied by the voids (C_v) remains constant during annealing, which, using the approach of Ref. 17 for H-induced voids, is estimated to be $C_v = 5\times10^{-9}$ cm^3/cm$^2 \pm 20\%$. Following Ref. 17, we believe that the temperature and time evolution of the voids can be explained as a conservative Ostwald ripening process which involves vacancy (V) diffusion from small voids to larger ones. There is strong evidence that the voids originate from, and develop by means of the evolution of, vacancies and (or) V-related defects; this is deduced from a comparative TEM study of samples after RTA at 900 °C for 30 s in oxygen or in nitrogen atmospheres (Table I). Oxidation of Si is a well-known powerful tool for the injection of non-equilibrium concentrations of self-interstitials (I) into the crystal;[18,19] it is therefore used as an indicator of the presence of V-related defects. It is estimated (Table I) that after RTA at 900 °C for 30 s in oxygen, the value of C_v is more than a factor of two smaller than the value obtained after RTA in nitrogen ($\sim 2.2\times10^{-9}$ cm^3/cm^2 in O_2 against $\sim 5.7\times10^{-9}$ cm^3/cm^2 in N_2). However, an even more important finding is the amazingly homogeneous size distribution of the voids (around 6–9 nm) in the case of oxidation as compared to the broad, and even bimodal (around 4–10 and 15–25 nm), void-size distribution in the case of nitrogen. The broad size distribution in the latter sample is most likely due to Ostwald ripening in the conditions of fast heating and rapid annealing. On the other hand, the homogeneous size distribution of the voids together with the reduced C_v value after RTA in the oxygen ambiance, strongly indicate that the vacancies, emitted by the small voids, more likely annihilate with the oxidation-induced self-interstitials and, therefore, do not reach and attach to the large voids.

Another interesting result of the defect evolution is presented in Fig. 3. Here, the samples implanted with Ge or As ions to identical conditions (energy, dose, temperature, and rate of MBE growth, etc.) and annealed by RTA at 800 °C for 30 s are compared. It is found that interstitial DLs and no voids are formed in the As implanted layers and voids and no

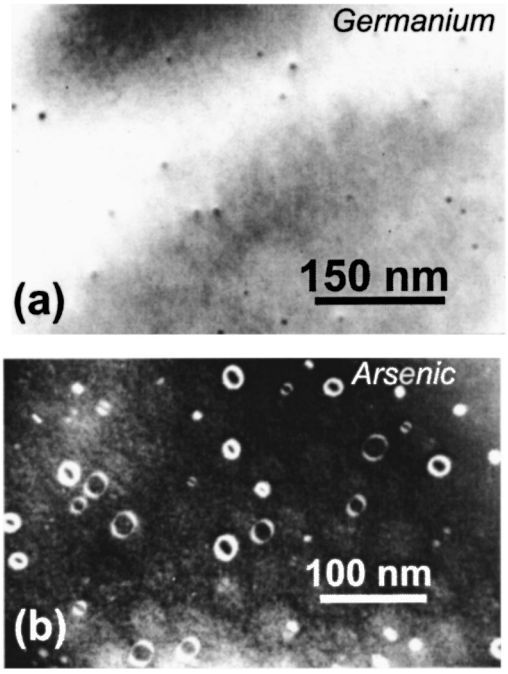

FIG. 3. Bright-field (a) and dark-field weak beam (b) TEM images of SiGe/Si structures which were in-situ implanted with Ge (a) or As (b) in identical conditions and annealed by RTA at 800 °C for 30 s.

DLs are formed in the Ge implanted layers. However, as determined by XTEM, both voids and DLs are entirely assembled within the implanted layer. Similar to the voids, the size of the DLs increases and their density decreases with increasing RTA temperature (Table I).

Figure 4 shows photoluminescence spectra, taken from the void-containing layers at different stages of their thermal evolution. In addition to the bound exciton transverse-optical (TO) emission originated from the substrate region, all spectra consist of a broad line located in the low-energy part of the PL spectrum at about 0.8–0.9 eV. The intensity of the PL line at 0.8–0.9 eV varies strongly with the anneal temperature. Being relatively low at $T<600\,^{\circ}\mathrm{C}$ and at $T>800\,^{\circ}\mathrm{C}$, the PL intensity of the 0.8–0.9 eV line increases enormously after an annealing between 700 and 750 °C (see the inset in Fig. 4). In this temperature range, the intensity of the 0.8–0.9-eV line is more than 20 times higher than the intensity of the TO line. For a reference, the dislocation-related lines $D1$ (0.807 eV), $D2$ (0.874 eV), and the TO line obtained in Si and SiGe/Si structures are similar in their intensities (see, e.g., Refs. 7 and 8). Second, it is clearly seen in Fig. 4 that the PL line at 0.8–0.9 eV shifts into the high-energy photon range when the annealing temperature increases and this correlates well with the increase of the void size. Finally, no evidence of similar behavior of the PL spectra is found in the case of As-ion implantation.

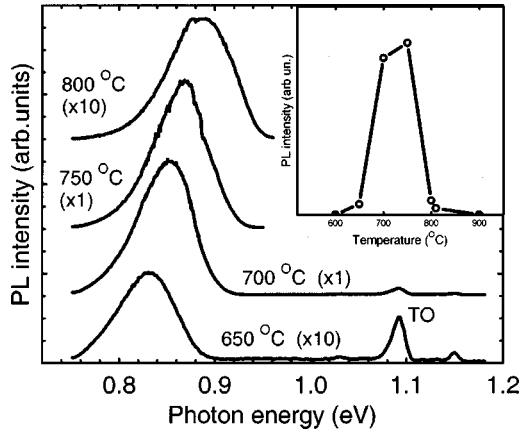

FIG. 4. PL spectra obtained at 4.2 K from the samples implanted with Ge ions and annealed at the indicated temperatures. The inset shows the temperature dependence of the yield of the 0.8–0.9-eV PL band. The spectra are scaled by the factors indicated in brackets.

The results of the PL measurements correlate well with the structure evolution which may indicate a vacancy cluster-(void-) assisted enhancement of the PL in the Ge implanted layers. In particular, the intensity of the PL is maximal in the temperature interval of 700–750 °C; a nucleation stage of the voids, probably through a condensation of vacancies and vacancy clusters, takes place in the same temperature range. This is well identified from a comparison of the PL and TEM data. Figure 5 presents the structures of the samples implanted with Ge and annealed in the temperature range of 600–750 °C. Compared to the as-grown samples, only insignificant modifications of the size, shape, and density of implantation induced defects take place during annealing at 600 °C [Figs. 1(a) and 5(a)]. A further increase of the temperature to 650 °C, however, results in significant growth of the largest point defect clusters at the expense of the smallest followed by defect coalescence into some kind of defect ensembles [Fig. 5(b)]. The next important stage is a threshold-like transformation of clusters of point defects to voids which happens in the temperature range between 700 and 750 °C [Figs. 5(c) and 5(d)]. The nucleation and growth of the voids is accompanied by the disappearance of the point defect clusters: both voids (bright spots of 5–7 nm large) and point defect clusters (fine granular background with a typical grain-size of about 1–3 nm in the TEM picture) simultaneously exist in the dark-field weak-beam TEM image in this case [Fig. 5(c)]. A further increase of the temperature to 750 °C results in a slight increase of both the size and density of the voids and in complete annealing of the point defect clusters. Thus, the comparison of Figs. 4 and 5 gives clear evidence that the enhancement of the PL yield correlates with the stage of void nucleation. If we suppose now that the nucleation of the voids and growth is mediated by a vacancy-related mechanism then the PL enhancement must be interpreted as being due to vacancy clusters or small voids. Similar to our recent investigations[6] we believe that a nonhomogeneous distribution of strain in the SiGe alloy layer around the incorporated vacancy-related defects is responsible for the observed PL enhancement. However, based on the present data this mechanism cannot be proven as the only possible one.

IV. DISCUSSION

Void formation has been studied extensively in Si and Ge after incorporation of hydrogen or noble gases.[17,20–23] In

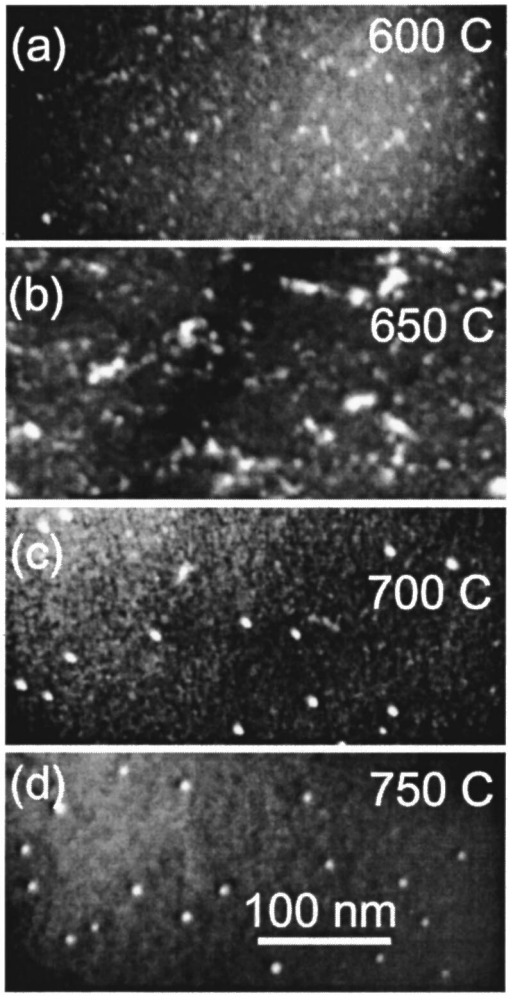

FIG. 5. Dark-field weak beam TEM images of Si/SiGe/Si structures which were *in situ* implanted with Ge and furnace annealed at 600 °C. (a), 650 °C (b), 700 °C (c), or 750 °C (d) for 10 min in a dry N_2 ambiance. Note that the main nucleation of voids and annealing of as-implanted defects take place in the temperature range 650–750 °C.

such samples, the evolution of the defects includes the successive formation of extended planar defects (so called ''platelets'') which transform to cylindrical and to spherical cavities[17] with increasing anneal temperature. It is assumed,[17,20–22] that the platelets accumulate (and store) a huge number of vacancies due to H-*V* (or He-*V*) interaction[20–22] followed by the formation of stable aggregates (e.g., VH_4).[21] In H-ion implanted samples, several sharp vibrational lines[24] indicated the existence of vacancies. Upon thermal treatment (above 500 °C) the hydrogen diffuse out of the layers and the platelets transform into cavities; this is accompanied by the exchange of H atoms and vacancies.[17]

Several papers have been published recently, reporting the investigations of MeV proton-, boron-, Si^+- or Ge^+-implanted Si in which the formation of *V*-related defects is demonstrated.[25–29] Recent deep level transient spectroscopy measurements[25] have revealed a spatial shift between vacancy and interstitial (C_sC_i) depth profiles in silicon, implanted with light projectiles (protons, boron) of MeV energies. In particular, in samples implanted with 6-MeV B ions a shift of about 500 nm was found.[25] Divacancies, which transform into large *V* clusters after 200 °C annealing, are observed in MeV self-implanted Si layers by positron annihilation spectrometry (PAS).[26] Similarly, the presence of defects comprising, on the average, at least two vacancies is observed in Si, implanted with 400-keV Ge^+ ions and annealed at 700 °C for 20 min.[27] The formation of *V*-related clusters is observed by PAS in the surface layer at a depth range less than the projected ion range, R_p, after MeV implantation at elevated temperatures (up to 450 °C).[28,29] In particular, a high efficiency of metallic atom gettering at a depth of $R_p/2$ has been attributed to open volume defects, *V*-related clusters or voids in Ref. 29. However, Kögler *et al.*[30] recently demonstrated by PAS that no *V*-like defects could be detected in Si self-implanted at 3.5 MeV to a dose of 5×10^{15} Si/cm^2, and annealed at $T>800$ °C. Instead, interstitial-type defects, thought responsible for the impurity gettering, were observed in the $R_p/2$ region using XTEM.[30]

A mechanism based on a kinematic separation of Frenkel pairs has been discussed to account for the observed spatial separation of vacancies and interstitials[25] and the vacancy excess within the region around $R_p/2$.[28] The mechanism seems to have reasons in the case of MeV implanted samples, where the *I* and *V* peak concentrations are well separated in the space[25] with a reduced *I*-*V* annihilation probability. In the present work, however, Ge and As ions were implanted at an elevated temperature and at an energy as low as 1 keV which prevent the kinematic spatial separation of *V* and *I*. The similar atomic masses of the Ge and As ions and the fact that the same doses were used ensured the production of comparable amounts and similar depth distributions of the as-implanted defects and dopants. Indeed, the defects, TEM-imaged in the layers as-implanted with Ge (Fig. 1) or As (see Ref. 6), are similar in type and density. Therefore, the very different evolution of the defects structures in the case of As- and Ge-implanted layers upon annealing cannot be explained by implantation induced defects. A mechanism related to their different chemical nature must be searched for. There has recently been given strong evidence that As_nV_m ($n=1...5, n=1,2$) clusters are energetically favored[31,32] over isolated As in highly doped Si. In particular, several specific effects of electrical activation,[33] diffusion,[34] and *V*-secondary defect interaction[15] can be explained in terms of *V*-dopant clusters formation. Very recent PAS measurements have evidenced the formation of As_3V and As_5V_2 clusters in highly doped Si depending on the annealing temperature.[35] We therefore suggest that the formation of the As_nV_m clusters is the most powerful channel for vacancy absorption in As implanted layers. Moreover, it is well known that Ge is not an efficient vacancy trap, and that the Ge-V pair anneals already at room temperature;[36] higher orders Ge_nV_m complexes have not been observed. Thus, the formation of Ge_nV_m complexes is not expected to be an efficient channel for vacancy absorption. This difference between arsenics and germaniums interaction with vacancies could be part of the explanation of the vacancy-void formation in the case of Ge implantation and the lack of vacancy-

void formation in the case of As implantation. An explanation of the fact that the voids assemble within the SiGe layer, as it can be well recognized from the XTEM image in Fig. 2(b), must be sought in the strain situation of the SiGe layer. The SiGe layer is compressively strained after growth before annealing and there is no indication that the layer has relaxed during the subsequent annealing. Thus, the assembly of the voids in the strained SiGe layer could be a strain-relieving phenomenon; similar effect has previously been demonstrated in the strained SiGe layers in which hydrogen-related voids partly relieve the strain.[23,37] We believe that at the first stage *the strain-induced (enhanced)* in-diffusion of the vacancies and their accumulation within the layer of SiGe takes place. This is then followed by void nucleation and growth at high annealing temperature.

The above considerations are confirmed by the correlation between the number of vacancies in the voids and the number of implanted dopant atoms. The volume occupied by the voids (C_v) is determined from the TEM data and presented in Table I. The total number of vacancies in the voids can be estimated by multiplication of C_v with the atomic density. If we suppose that the composition of the layer which contain the voids is about $Si_{0.5}Ge_{0.5}$, and the atomic density is 4.7×10^{22} cm^{-2} (the composition of the SiGe layer might be slightly different from $Si_{0.5}Ge_{0.5}$ due to alloying at high RTA temperature) then the number of vacancies in the voids is about $(1-3)\times 10^{14}$ cm^{-2}. This value is much lower than that deduced from TRIM95 calculations[38] for ion-induced vacancy production, but is very close to the number of implanted dopant atoms. On the other hand, the estimation of the total vacancy production during ion implantation is not a simple task. First, the temperature of implantation was 520 °C which gives rise to effective dynamical (i.e., *in situ*) annealing of vacancies and interstitials.[39] Second, the energy of implantation was 1 keV, and according to TRIM95 calculations this corresponds to a mean range of about 2.7 nm and to a maximum nuclear energy deposition depth (zone of the interstitial-vacancy generation) of 1 nm. It is therefore natural to suppose that most of the interstitials and vacancies diffuse to the surface during irradiation. The vacancies, however, can be partially trapped and accumulated within the SiGe layer due to the compressive strain. In this case the number of interstitials might be lower as compared to the number of vacancies. In addition, the vacancy and interstitial population may strongly depend on the chemical nature of implanted dopant. As already mentioned, instead of the same implantation conditions (energy, dose, temperature) and of the similar atomic masses of the Ge and As ions, the very different evolution of the defect structures is registered which cannot be explained by implantation induced defects. Finally, the results of Holland *et al.*,[40] should be noted, where the formation of voids was observed in arsenic-but not in germanium-implanted Si layers. Their results are connected with lattice damage in Si during ion irradiation at *extreme dose and temperature* conditions as well as related to the vacancy-interstitial spatial separation due to the high energy of the implants. We believe that their irradiation conditions are not comparable with the conditions of our investigation due to possible chemical and high-dose effects (precipitation, large defect complexes, etc.).

V. SUMMARY

In conclusion, spherically shaped nanovoids are produced in MBE grown SiGe alloy layers with *in situ* implantation of low-energy Ge ions followed by thermal treatment at temperatures above ~750 °C, the nanovoids grow in size with increasing anneal temperature and are stable up to 900 °C. The nucleation stage of the voids is accompanied by a strong enhancement of the photoluminescence yield in the range of 1.4–1.55 μm. The PL enhancement is assumed to originate from the SiGe alloy layer which contains of vacancy-related point defect clusters, which are the main building material for the voids. Use of As as implantation species at the same conditions does not result in void formation but in regular interstitial dislocation loops. The difference in arsenics and germaniums interactions with vacancies is suggested to be responsible for this phenomenon.

ACKNOWLEDGMENT

We acknowledge the support by the Danish Strategic Material Research Program.

*Corresponding author. Electronic address: gaiduk@ifa.au.dk

[1] *Advances in Microcrystalline and Nonocrystalline Semiconductor*, edited by R. W. Collins, F. M. Fauchet, I. Shimizu, J. C. Vital, T. Shimada, and A. P. Alivisators, MRS Symposia Proceedings, Mater. Res. Soc. Symp. No. 452 (Materials Research Society, Pittsburgh, 1997).

[2] L. Rebohle, J. von Borany, H. Frob, and W. Skorupa, Appl. Phys. B: Lasers Opt. **71**, 131 (2000).

[3] L. T. Canham, Appl. Phys. Lett. **57**, 1046 (1990).

[4] S. Coffa, G. Franzo, and F. Priolo, MRS Bull. **23**, 25 (1998).

[5] O. G. Schmidt and K. Eberl, Phys. Rev. B **61**, 13721 (2000).

[6] P. I. Gaiduk, A. Nylandsted Larsen, J. Lundsgaard Hansen, A. V. Mudryi, M. P. Samtsov, and A. N. Demenschenok, Appl. Phys. Lett. **79**, 4025 (2001).

[7] V. V. Kveder, E. A. Steinmann, S. A. Shevchenko, and H. G. Grimmeiss, Phys. Rev. B **51**, 10520 (1995); V. V. Kveder, E. A. Steinman, and H. G. Grimmeiss, J. Appl. Phys. **78**, 446 (1995); E. A. Steinman, V. I. Vdovin, T. G. Yugova, V. S. Avrutin, and N. F. Izyumskaya, Semicond. Sci. Technol. **14**, 582 (1999).

[8] E. O. Sveinbjornsson and J. Weber, Appl. Phys. Lett. **69**, 2686 (1996).

[9] Wai Lek Ng, M. A. Lourenço, R. M. Gwilliam, S. Ledain, G. Shao, and K. P. Homewood, Nature (London) **410**, 192 (2001).

[10] M. A. Green, J. Shao, A. Wang, P. J. Reece, and M. Gal, Nature (London) **412**, 805 (2001).

[11] P. I. Gaiduk, J. Lundsgaard Hansen, and A. Nylandsted Larsen, Appl. Phys. A: Mater. Sci. Process. **73**, 761 (2001).

[12] P. I. Gaiduk, A. Nylandsted Larsen, and J. Lundsgaard Hansen, Appl. Phys. Lett. **79**, 3494 (2001).

[13] A. Agarwal, T. E. Haynes, D. J. Eaglesham, H. J. Gossmann, D. C. Jacobson, J. M. Poate, and Y. E. Erokhin, Appl. Phys. Lett. **70**, 3332 (1997).

[14] M. Bauer, M. Oehme, K. Lyutovich, and E. Kasper, Thin Solid Films **336**, 104 (1998).
[15] P. I. Gaiduk and A. Nylandsted Larsen, J. Appl. Phys. **68**, 5081 (1990).
[16] M. Ruhle and M. Wilkens, Cryst. Lattice Defects **6**, 129 (1975); M. H. Loretto, *Electron Beam Analysis of Materials* (Chaptmann and Hall, New York, 1988). P. B. Hirsch, A. Howie, R. B. Nicholson, D. W. Pashley, and M. J. Whelan, *Electron Microscopy of Thin Crystals* (Butterworths, London, 1965).
[17] J. Grisolia, F. Cristiano, G. Ben Assayang, and A. Claverie, Nucl. Instrum. Methods Phys. Res. B **178**, 160 (2001).
[18] S. M. Hu, Mater. Sci. Eng., R. **13**, 105 (1994).
[19] P. M. Fahey, P. B. Griffin, and J. D. Plummer, Rev. Mod. Phys. **61**, 289 (1989).
[20] V. Raineri, S. Coffa, E. Szilagyi, J. Gyulai, and E. Rimini, Phys. Rev. B **61**, 937 (2000).
[21] F. A. Reboredo, M. Ferconi, and S. T. Pantelides, Phys. Rev. Lett. **82**, 4870 (1999).
[22] B. Bech Nielsen, L. Hoffmann, and M. Budde, Mater. Sci. Eng., B **36**, 259 (1996).
[23] B. Hollander, St. Lenk, S. Mantl, H. Trinkaus, D. Kirch, M. Luysberg, T. Hackbarth, H. J. Herzog, and P. F. P. Fichtner, Nucl. Instrum. Methods Phys. Res. B **175**, 357 (2001).
[24] M. K. Weldon, V. E. Marsico, Y. J. Chabal, A. Agarwal, D. J. Eaglesham, J. Sapjeta, W. L. Brown, D. C. Jacobson, Y. Caudano, S. B. Christman, and E. E. Chaban, J. Vac. Sci. Technol. B **15**, 1065 (1997).
[25] P. Pellegrino, P. Leveque, J. Wong-Leung, C. Jagadish, and B. G. Svensson, Appl. Phys. Lett. **78**, 3442 (2001); P. Pellegrino, H. Kortegaard-Nielsen, A. Hallen, J. Wong-Leung, C. Jagadish, and B. G. Svensson, Nucl. Instrum. Methods Phys. Res. B **186**, 334 (2002).
[26] B. Nielsen, O. W. Holland, T. C. Leung, and K. G. Lynn, J. Appl. Phys. **74**, 1636 (1993).
[27] S. A. E. Kuna, P. G. Coleman, A. Nejim, F. Cristiano, and P. L. Hemment, Semicond. Sci. Technol. **13**, 394 (1998).
[28] O. W. Holland, J. D. Budai, and B. Nielsen, Mater. Sci. Eng., A **253**, 240 (1998).
[29] G. A. Rozgonyi, J. M. Glasko, K. L. Beaman, and S. V. Koveshnikov, Mater. Sci. Eng., B **72**, 87 (2000).
[30] R. Kögler, A. Peeva, W. Anwand, G. Brauer, W. Skorupa, P. Werner, and U. Gösele, Appl. Phys. Lett. **75**, 1279 (1999).
[31] M. Ramamoorthy and S. T. Pantelides, Phys. Rev. Lett. **76**, 4753 (1996).
[32] M. A. Berding and A. Sher, Phys. Rev. B **58**, 3853 (1998).
[33] A. Nylandsted Larsen, B. Christensen, and S. Yu. Shiryaev, J. Appl. Phys. **71**, 4854 (1992).
[34] A. Nylandsted Larsen, K. Kyllesbech Larsen, P. E. Andersen, and B. G. Svensson, J. Appl. Phys. **73**, 691 (1993).
[35] V. Ranki, K. Saarinen, J. Fage-Pedersen, J. Lundsgaard Hansen, and A. Nylandsted Larsen, Phys. Rev. B **67**, 041201 (2003).
[36] G. D. Watkins, in *Deep Centers in Semiconductors*, edited by S. T. Pantelides (Gordon and Breach, New York, 1986), p. 147.
[37] P. I. Gaiduk, A. Nylandsted Larsen, J. Lundsgaard Hansen, and F. F. Komarov, Vacuum Techn. and Technology, 1999, Vol. 123, pp. 55–59.
[38] J. F. Ziegler, J. P. Biersack, and U. Littmark, *The Stopping and Range of Ions in Solids* (Pergamon, New York, 1985).
[39] J. P. Souza and D. K. Sadana, in *Handbook on Semiconductors*, Vol. 36, *Materials, Properties and Preparation*, edited by T. S. Moos (North-Holland, Amsterdam, 1994), p. 203.
[40] O. W. Holland, L. Xie, B. Nielsen, and D. S. Zhou, J. Electron. Mater. **25**, 99 (1996).